Journal of Physics: Conference Series **497** (2014) 012028 doi:10.1088/1742-6596/497/1/012028

Collective modes of three- and two-dimensional trapped Fermi gases in the normal phase

M. Urban[1], S. Chiacchiera[2], D. Davesne[3], T. Enss[4] and P.-A. Pantel[3]

[1] Institut de Physique Nucléaire, CNRS/IN2P3 and Univ. Paris Sud, 91406 Orsay cedex, France

[2] Centro de Física Computacional, Department of Physics, University of Coimbra, 3004-516 Coimbra, Portugal

[3] IPN Lyon, Université de Lyon, Université Lyon 1, CNRS/IN2P3, 69622 Villeurbanne cedex, France

[4] Institut für Theoretische Physik, Universität Heidelberg, D-69120 Heidelberg, Germany

E-mail: urban@ipno.in2p3.fr

Abstract. We study the transition from the hydrodynamic to the collisionless regime in collective modes of three- and two-dimensional Fermi gases by using the semiclassical Boltzmann equation. We use direct numerical simulations as well as the method of phase-space moments to solve the Boltzmann equation and show that the restriction to second-order moments is not accurate enough. By including higher-order moments, we can successfully describe the hydrodynamic to collisionless transition observed in the quadrupole mode in three-dimensional Fermi gases and the frequency shift and damping of the sloshing mode due to the anharmonic shape of the experimental trap potential. In the case of two-dimensional Fermi gases, however, the strong damping of the quadrupole mode observed in a recent experiment remains unexplained.

1. Introduction

By studying collective motion in ultracold atoms, one can address some questions that cannot be answered from the measurement of static (equilibrium) quantities alone. Concentrating here on the case of unpolarized Fermi gases, let us mention the superfluid-normal phase transition, which can be seen most convincingly by looking at vortices in rotating traps [1]. It also shows up, somewhat less impressively, in the radial quadrupole mode [2, 3]. Also in the normal phase, above the critical temperature, Fermi gases in the strongly interacting regime reveal interesting dynamical properties. For instance, in the anisotropic expansion of normal-fluid Fermi gases in the unitary limit (i.e., exactly on a Feshbach resonance, where the scattering length a diverges) it was observed that the viscosity of these systems is surprisingly low [4]. With increasing temperature, however, the system expands, gets more and more dilute, and finally it becomes essentially collisionless [5]. As one approaches the collisionless regime, the concept of viscous hydrodynamics breaks down and a more microscopic description in the framework of the Boltzmann equation is needed.

In the present work we concentrate on collective oscillations with small amplitude. Some of these collective modes are depicted schematically in Fig. 1. The first one (a) is the sloshing mode, an oscillation of the atom cloud as a whole with the trap frequency. This mode is very

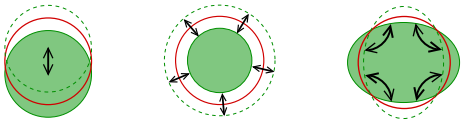

Figure 1. Schematic representation of different collective modes, as seen in the xy plane: (a) sloshing mode, (b) breathing mode, (c) radial quadrupole mode.

useful since it allows the experimentalists to determine the trap frequency. However, as discussed later, in a realistic (Gaussian) trap one has to be careful to account for anharmonicity effects. The second example (b) shows the radial breathing mode. Breathing modes are of interest because they give information about the equation of state. While in the usual three-dimensional traps the axial breathing mode behaves always hydrodynamically because of its low frequency, the frequency and damping rate of the radial breathing mode are sensitive to the transition from the hydrodynamic to the collisionless regime. This is even more pronounced in the case of the radial quadrupole mode (c), whose frequency changes from $\sqrt{2}\omega_r$ (ω_r being the radial trap frequency) in the hydrodynamic limit to approximately $2\omega_r$ in the collisionless limit. The damping is maximal in the intermediate regime between the two limits.

2. Formalism

We consider a two-component $(\uparrow,\downarrow)$ Fermi gas with equal distribution functions $f_\uparrow(\mathbf{r},\mathbf{p},t) = f_\downarrow(\mathbf{r},\mathbf{p},t) = f(\mathbf{r},\mathbf{p},t)$. The Boltzmann equation describing the time dependence of the common distribution function $f(\mathbf{r},\mathbf{p},t)$ reads

$$\dot{f} + \frac{\mathbf{p}}{m}\cdot\boldsymbol{\nabla}_r f - \boldsymbol{\nabla}_r V\cdot\boldsymbol{\nabla}_p f = -I[f] \tag{1}$$

where m is the atom mass, $V(\mathbf{r}) = V_{trap}(\mathbf{r}) + U(\mathbf{r})$ is the sum of trap potential and mean field. The mean field $U(\mathbf{r})$ is obtained in local-density from the real part of the self-energy, $\mathrm{Re}\,\Sigma$, calculated in ladder approximation (see Fig. 2) [6]. The collision term I on the rhs. of Eq. (1) reads

$$I[f] = \int \frac{d^3p_1}{(2\pi\hbar)^3}\int d\Omega \frac{d\sigma}{d\Omega}\,|\mathbf{v}-\mathbf{v}_1|\,(f f_1 \bar{f}'\bar{f}_1' - f' f_1' \bar{f}\bar{f}_1) \tag{2}$$

where the factors $\bar{f} = (1-f)$ etc. are included to take Pauli blocking into account, $\mathbf{v}-\mathbf{v}_1$ is the relative velocity of the two colliding atoms. The cross section σ is obtained from the absolute square of the in-medium T matrix (see Fig 2). At low temperature, the in-medium cross section σ is strongly enhanced compared to the free-space one, $\sigma_{\mathrm{free}} = 4\pi a^2/[1+(qa)^2]$, especially for head-on collisions ($\mathbf{p}_1 \sim -\mathbf{p}$) with $|\mathbf{p}| \sim |\mathbf{p}_1| \sim k_F$. This can be interpreted as a precursor effect of the pole in the T matrix at $T = T_c$ [6, 7]. (The same effect was found in nuclear physics, cf. [8]).

In Eq. (2), the collision term is written for the three-dimensional case. In two dimensions one just has to replace the integral over $d^3p_1 d\Omega$ (Ω being the solid angle characterizing the direction of $\mathbf{p}'$) by an integral over $d^2p_1 d\theta$ (θ being the scattering angle). The enhancement of the in-medium cross section compared to the free-space one is also found in two dimensions.

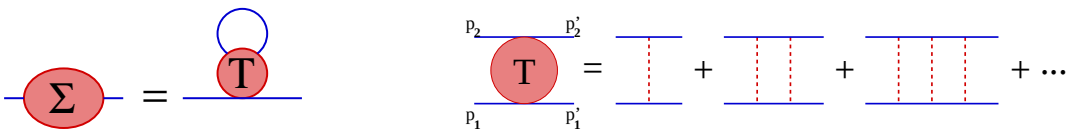

Figure 2. Feynman diagrams for the self-energy (left) and the in-medium T matrix (right) in ladder approximation.

In practice, we employ two different methods to solve Eq. (1). The first one is a numerical simulation where the continuous function $f(\mathbf{r}, \mathbf{p}, t)$ is replaced by a set of delta functions, the so-called test particles. So far, test-particle calculations in the context of cold atoms [9, 10, 11] have not included the mean field U and the medium modified cross section. The main difficulty is that it takes too much computation time to evaluate the in-medium cross section for each pair of possibly colliding test particles. We are presently working on a solution of this problem by combining analytical expressions for the in-medium cross section obtained in a high-temperature expansion with a parametrization fitted to the full cross-section at low temperatures. The test-particle results discussed here were obtained with the free cross section.

The second method is the method of moments. For small oscillations, the distribution function can be written in the form

$$f(\mathbf{r}, \mathbf{p}, t) = f_{\rm eq}(\mathbf{r}, \mathbf{p}) + \frac{df_{\rm eq}}{d\mu}\, \Phi(\mathbf{r}, \mathbf{p}, t) \tag{3}$$

where $f_{\rm eq}$ denotes the distribution function in equilibrium, i.e., the Fermi function with chemical potential μ, and Φ is a smooth function. We make the ansatz

$$\Phi(\mathbf{r}, \mathbf{p}, t) = \sum_{i=1}^{n} c_i(t)\phi_i(\mathbf{r}, \mathbf{p})\,, \tag{4}$$

where ϕ_i are monomials in $\mathbf{r}$ and $\mathbf{p}$ and c_i are time-dependent coefficients. We linearize the Boltzmann equation, i.e., we keep only first-order terms in Φ. By taking phase-space moments of this linearized equation, i.e., by multiplying it by each of the ϕ_i and integrating over phase space, we obtain a system of n linear equations of motion for the coefficients c_i which can easily be solved by matrix diagonalization.

3. Importance of higher-order moments

Often only the minimal set of functions ϕ_i necessary for the description of a collective mode [6, 12, 13] is used. For instance, for the breathing, quadrupole, and scissors modes, one needs second-order terms to describe the oscillation of the system shape in coordinate (e.g., $\phi_1 = xy$) and momentum space (e.g., $\phi_2 = p_x p_y$) and of the velocity field (e.g., $\phi_3 = xp_y$, $\phi_4 = yp_x$), while the simplest possible sloshing motion requires only first-order terms ($\phi_1 = x$, $\phi_2 = p_x$). However, it is important to check quantitatively how strong the corrections due to higher-order moments are.

In Fig. 3 we display a comparison between the test-particle method [10] and the method of moments at second and fourth order for the case of the quadrupole mode in a spherical trap. The peak position corresponds to the quadrupole frequency, while the width defines the

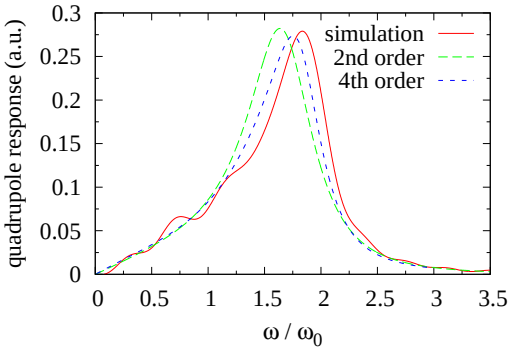

Figure 3. Quadrupole response as a function of the excitation frequency ω, obtained by a test particle simulation and by the moments method including up to second- and up to fourth-order terms [10]. The calculations were done for $N = 10^4$ atoms in a spherical trap (frequency ω_0), temperature $T/T_F = 0.4$, interaction parameter $1/k_F a = -0.5$, with the free-space cross section and without mean field.

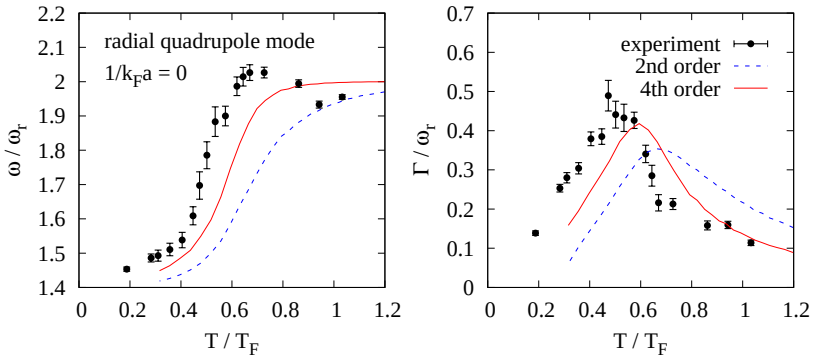

Figure 4. Frequency ω and damping rate Γ of the radial quadrupole mode as functions of temperature. The data and system parameters are taken from Ref. [13], the theoretical curves were obtained within the second- and fourth-order moments method, respectively [14].

damping rate. It can be seen that the inclusion of fourth-order moments improves significantly the agreement between the moments method and the test-particle calculation.

We also applied the fourth-order moments method to a realistic case studied in a ^{6}Li experiment at Innsbruck [13]. In this calculation [14], the medium modification of the cross section was taken into account. As an example, we display in Fig. 4 the frequency and damping rate of the quadrupole mode as functions of the temperature, obtained within the method of moments at second and fourth order, together with the experimental data. One can clearly see the smooth transition from hydrodynamic to collisionless behavior as the temperature increases. The reason is that the collision rate decreases when the gas expands and becomes more dilute at high temperature. As one can see, the second-order results overestimate the collision effects and therefore reach the collisionless regime at too high temperatures. The extension of the moments method to fourth-order terms clearly improves the agreement with the data. However, we mention that in the case of the scissors modes we did not find a clear improvement due to the inclusion of fourth-order terms [14].

4. Sloshing mode in an anharmonic trap

In a harmonic trap, the sloshing mode is an undamped center-of-mass oscillation of the atom cloud as a whole, leaving the shape of the atom cloud unchanged (Kohn theorem [15]). Since its frequency is that of the trap, independently of the interaction and other system parameters, it is very interesting for experimentalists for the precise determination of the trap frequency.

In real experiments, however, the trap potentials have more or less pronounced anharmonicities. For instance, in an optical trap, where the radial confinement is produced by a laser beam with waist w, the trap potential in radial direction is of the form $V_{\rm trap}(r_\perp) \sim -V_0 \exp(-2r_\perp^2/w^2)$. Only if the particle energies (i.e., Fermi energy E_F and temperature T) are much smaller than the trap depth V_0, this potential can be considered as approximately harmonic. The anharmonicity of the potential changes the sloshing frequency, $\omega_{\rm slosh} \neq \omega_r$ [if we define the radial trap frequency ω_r by $\omega_r^2 = (1/m)(d^2V_{\rm trap}/dr_\perp^2)_{r_\perp=0}$] and leads also to a damping of the sloshing mode.

We studied the sloshing mode within the method of moments for the parameters of the experiment [13]. The main results of Ref. [16] are summarized in Fig. 5. With increasing temperature the cloud expands and extends more and more into the anharmonic region of the trap, where the trap potential is weaker than the idealized harmonic potential. Therefore, the sloshing frequency (left panel of Fig. 5) decreases, as it is observed in the experiment. The general trend is correctly reproduced by the moments method at first and at third order. Also the mean field has only a weak effect. When comparing with the experimental data, however, one should note that in the normalization of the experimental data it was assumed that the sloshing frequency extrapolated to $T = 0$ should be equal to the trap frequency, which explains why the data are shifted upwards as compared to the theoretical results.

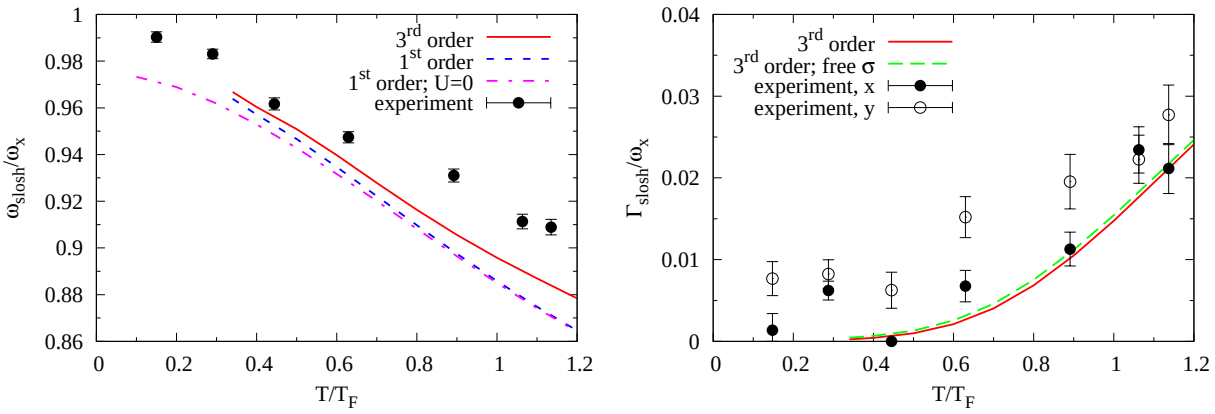

Figure 5. Left: temperature dependence of the sloshing frequency in the experiment [13] and theoretical results [16] obtained within the moments method up to third (solid line) and first order (dashes), respectively. For comparison, also the first-order result obtained without mean field ($U = 0$) is shown (dashed-dotted curve). Right: corresponding damping of the sloshing mode within the third-order moments method (solid line). For comparison, also the result obtained with the free-space cross section (free σ, dashes) is shown. The data are from [17].

While the inclusion of third-order moments does not have a dramatic effect on the sloshing frequency, it is crucial for the calculation of the damping rate of the sloshing mode. Within the first-order moments method, the sloshing mode is undamped because x and p_x are conserved during a collision. In order to describe the damping, one has to include at least third-order terms such as x^3, xy^2, xp_x^2, xp_y^2, etc. (in total, Φ contains now 18 terms [16]). As shown in the right panel of Fig. 5, the resulting damping is still very weak and it is compatible with the experiment. We note that it practically does not matter if we use the in-medium or the free-space cross section in this calculation.

In our calculation, the origin of the damping is that, as the cloud oscillates in the anharmonic potential, its form changes. This leads to deformations of the Fermi sphere in momentum space, which are damped by collisions. The change of the system shape during the sloshing motion can also be interpreted in the following way: already in a harmonic trap, there are in addition to the sloshing mode more complicated (i.e., described by moments of higher order) dipolar collective modes which are damped. The anharmonicity leads to a coupling between the sloshing mode and these higher-order modes. As examples, we display in Fig. 6 the velocity fields of the modes excited by the operators $(x^2 + y^2 - 2\langle r_\perp^2 \rangle_{\rm eq})x$ (compressional dipole mode in the xy plane) and $(z^2 - \langle z^2 \rangle_{\rm eq})x$ ("bending mode" in the xz plane).

5. Anharmonicity effects in the quadrupole mode in two dimensions

In a recent ^{40}K experiment done at Cambrigde [18, 19], the frequency and damping of the quadrupole mode in two dimensions were studied. Although the analysis made in [19] based on second-order moments could explain the transition of the observed frequency of the quadrupole mode from the hydrodynamic to the collisionless regime with decreasing interaction strength [increasing $\ln(k_F a_{2D})$], there was an unexplained offset in the damping rate. Since this unexplained damping persisted even in the non-interacting regime, it was reasonable to assume that it was caused by anharmonicity effects.

In fact, the experimental trap potential (see [20] for details) is not only anharmonic like an inverted Gaussian, it also has a small ellipticity and it is deformed by linear terms due to gravity and magnetic field gradients which destroy the symmetry of the potential, i.e.,

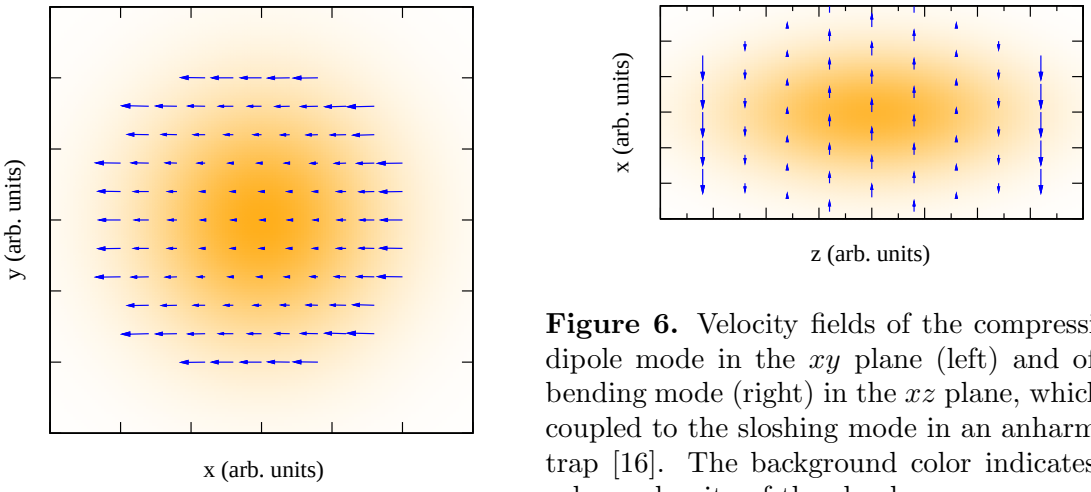

Figure 6. Velocity fields of the compressional dipole mode in the xy plane (left) and of the bending mode (right) in the xz plane, which are coupled to the sloshing mode in an anharmonic trap [16]. The background color indicates the column density of the cloud.

$V_{\rm trap}(-\mathbf{r}) \neq V_{\rm trap}(\mathbf{r})$. The model potential we used in our analysis [21] is shown in Fig. 7. As a consequence of the asymmetric shape of the potential, modes of different symmetries (such as sloshing, breathing, and quadrupole modes) are coupled to one another. In order to take this coupling into account, we included in our analysis all moments up to fourth order, i.e., all terms of the form $x^i y^j p_x^k p_y^l$ where i, j, k, l are non-negative integer numbers with $i+j+k+l \leq 4$ (70 terms in total) [21]. In our calculation, we include the in-medium cross section but not the mean field.

In Fig. 8 we compare our results for the frequency and damping rate of the quadrupole mode with the experimental ones. The results are shown as functions of the parameter $\ln(k_F a_{2D})$ characterizing the interaction strength, large values of $\ln(k_F a_{2D})$ corresponding to weak interaction. The frequency tends to the hydrodynamic one ($\sqrt{2}\omega_r$) in the limit of small $\ln(k_F a_{2D})$ and to the collisionless one ($2\omega_r$) in the limit of large $\ln(k_F a_{2D})$. We start with the simplest model, namely an isotropic harmonic potential (a) and include one by one the different imperfections of the realistic potential: ellipticity (b), anharmonicity (c), linear terms due to gravity and magnetic field gradients (d). It can be seen that these details have only little effect on the results: in this experiment the harmonic approximation is actually very good because the Fermi energy is small compared to the trap depth. In particular, the damping that persists in the weakly interacting regime cannot be explained by anharmonicity effects.

We note that the effect of higher-order moments is much weaker here than in the three-dimensional case discussed in Sec. 3. We thus confirm the results obtained in the analysis of

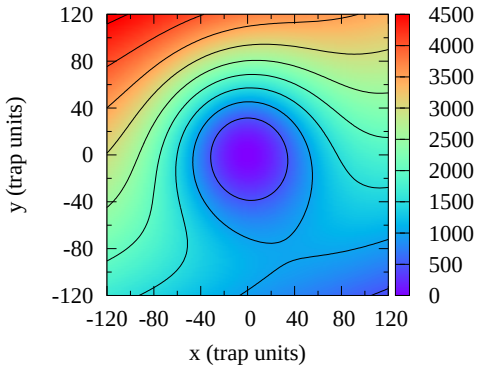

Figure 7. Contour plot of the model potential to describe the two-dimensional experiment of Refs. [18, 19]. The potential is shown in units of $\hbar\omega_r$ (ω_r being the trap frequency) as function of x and y in units of the oscillator length $l_{\rm ho} = \sqrt{\hbar/m\omega_r}$.

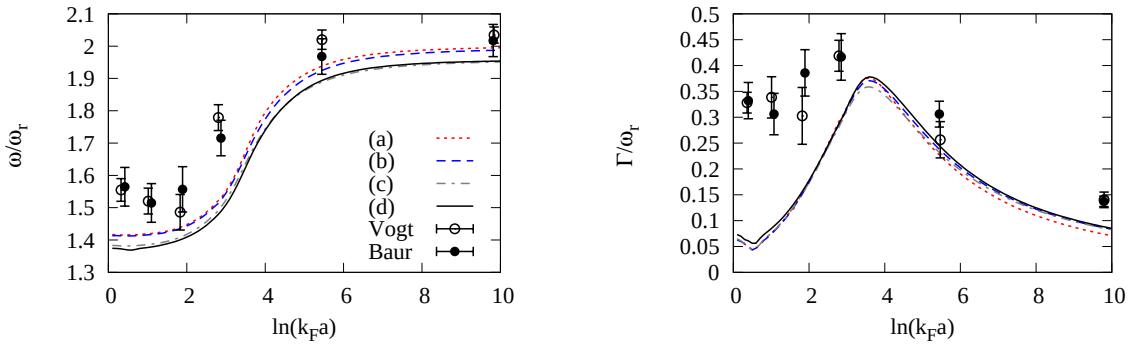

Figure 8. Frequency ω and damping rate Γ of the quadrupole mode as functions of the interaction strength (for $N = 4300$ atoms at $T = 0.47T_F$ in a two-dimensional trap). Theoretical results obtained with fourth-order moments [21] are compared with experimental data from Vogt et al. [18] and Baur et al. [19], respectively. The curves (a)–(d) correspond to different approximations of the realistic trap potential (see text).

[19] within the second-order moments method.

In contrast to what was found in an estimate based on a calculation of the shear viscosity [22], also the in-medium enhancement of the cross section has only a moderate effect on the damping. This finding, which is in agreement with the results of [19], is again very different from the three-dimensional case discussed in Sec. 3. The fact that the theory cannot explain the strong damping observed experimentally in the strongly-interacting regime [$\ln(k_F a_{2D}) \lesssim 1$] is maybe due to the breakdown of the validity of the Boltzmann equation in this regime.

6. Summary

We have studied various aspects of collective modes of trapped Fermi gases in the normal-fluid phase. The Boltzmann equation allows us to describe the transition from hydrodynamic to collisionless behavior, which is observed in both three- and two-dimensional systems. The method of moments was used to obtain approximate solutions of the linearized Boltzmann equation in the limit of small oscillations around equilibrium.

By comparing with a direct numerical solution within the test-particle method, we found that the moments method including only second-order moments overestimates the collisional effects in the case of the quadrupole mode in a spherical trap. By including also fourth-order moments, the agreement improves a lot. Also the results for the radial quadrupole mode in an elongated trap are in better agreement with experimental results if fourth-order moments are included.

Within the higher-order moments method, we were able to explain the experimentally observed damping of the sloshing mode in an anharmonic three-dimensional trap. Here the necessity to include higher-order moments (third order in this case) is obvious since at lowest order (first order) the sloshing mode is undamped.

We also studied the effects of a realistic anharmonic potential on the damping of the quadrupole mode in two dimensions. It turned out that the anharmonicity effects are by far too weak to explain the experimentally observed damping in the weakly interacting regime. It seems that the effect of higher-order moments is less important in two dimensions than in the three-dimensional cases discussed before.

It should be mentioned that the strong damping of the quadrupole mode near the superfluid-normal phase transition, observed in both two- and three-dimensional systems, still lacks a theoretical description. Probably the Boltzmann equation is not applicable in this regime.

Interesting subjects for future studies are the inclusion of the in-medium cross section and mean-field into numerical test-particle simulations, which so far have been limited to the free cross section without mean field. Work in this direction is in progress. The description of spin modes and modes in imbalanced Fermi gases is more difficult since it requires a model for the cross section and for the mean field in the imbalanced case, which is non-trivial because of the failure of the usual ladder approximation in this case [23, 24, 25].

References

[1] Schunck C H, Zwierlein M W, Schirotzek A and Ketterle W 2007 *Phys. Rev. Lett.* **98** 050404
[2] Altmeyer A, Riedl S, Wright M J, Kohstall C, Denschlag J H and Grimm R 2007 *Phys. Rev.* A **76** 033610
[3] Urban M 2008 *Phys. Rev.* A **78** 053619
[4] Cao C, Elliott E, Joseph J, Wu H, Petricka J, Schäfer T and Thomas J E 2011 *Science* **331** 58
[5] Wright M J, Riedl S, Altmeyer A, Kohstall C, Sánchez Guajardo E R, Hecker Denschlag J and Grimm R 2007 *Phys. Rev. Lett.* **99** 150403
[6] Chiacchiera S, Lepers T, Davesne D and Urban M 2009 *Phys. Rev.* A **79** 033613
[7] Bruun G M and Smith H 2005 *Phys. Rev.* A **72**, 043605
[8] Alm T, Röpke G and Schmidt M 1994 *Phys. Rev.* C **50** 31
[9] Toschi F, Vignolo P, Succi S and Tosi M P 2003 *Phys. Rev.* A **67** 041605
[10] Lepers T, Davesne D, Chiacchiera S and Urban M 2010 *Phys. Rev.* A **82** 023609
[11] Goulko O, Chevy F and Lobo C 2011 *Phys. Rev.* A **84** 051605
[12] Bruun G M and Smith H 2007 *Phys. Rev.* A **76**, 045602
[13] Riedl S, Sánchez Guajardo E R, Kohstall C, Altmeyer A, Wright M J, Hecker Denschlag J, Grimm R, Bruun G M and Smith H 2008 *Phys. Rev.* A **78** 053609
[14] Chiacchiera S, Lepers T, Davesne D, Urban M 2011 *Phys. Rev.* A **84** 043634
[15] Kohn W 1961 *Phys. Rev.* **123** 1242
[16] Pantel P-A, Davesne D, Chiacchiera S and Urban M 2012 *Phys. Rev.* A **86** 023635
[17] Sidorenkov L and Grimm R 2012 (unpublished)
[18] Vogt E, Feld M, Fröhlich B, Pertot D, Koschorreck M and Köhl M 2012 *Phys. Rev. Lett.* **108** 070404
[19] Baur S, Vogt E, Köhl M and Bruun G M 2013 *Phys. Rev.* A **87** 043612
[20] E. Vogt 2013 PhD Thesis (University of Cambridge)
[21] Chiacchiera S, Davesne D, Enss T and Urban M 2013 *Phys. Rev.* A **88** 053616
[22] Enss T, Küppersbusch C and Fritz L 2012 *Phys. Rev.* A **86** 013617
[23] Xia-Ji Liu and Hui Hu 2006 *Europhys. Lett.* **75** 364
[24] Parish M M, Marchetti F M, Lamacraft A and Simons B D 2007 *Nature Phys.* **3** 124
[25] Kashimura T, Watanabe R and Ohashi Y 2012 *Phys. Rev.* A **86** 043622